A theory on the x-ray sensitivity of a silicon surface-barrier detector including a thermal charge-diffusion effect

T. Cho, M. Hirata, E. Takahashi, T. Teraji, N. Yamaguchi, K. Matsuda, A. Takeuchi, J. Kohagura, K. Ogura,[a] T. Kondoh,[b] A. Osawa,[c] K. Yatsu, T. Tamano, and S. Miyoshi
Plasma Research Center, University of Tsukuba, Tsukuba, Ibaraki 305, Japan

(Received 2 January 1992; accepted for publication 22 June 1992)

An analytical method based on a new theoretical model for the x-ray energy responses of silicon surface-barrier (SSB) detectors has been proposed. This method may address a recent confusing issue in the x-ray detection characteristics of SSB semiconductor detectors; that is, the x-ray responses of SSB detectors as well as *p-i-n* diodes used in underbiased operations were recently found to be contrary to the commonly held belief that the x-ray sensitivity of an SSB detector is determined by the thickness of the depletion layer. The model presented includes a signal contribution from thermally diffusing charge that is created in the field-free substrate region within a diffusion length from the depletion layer along with a signal contribution from charge created in the depletion layer. This model predicts a large signal contribution from the charge-diffusion effect on the SSB responses to high-energy x rays. Formulas and calculated results supporting SSB calibration data have been represented. These analytical methods might be developed to apply the analyses and predictions of energy responses of various types of silicon detectors including *p-i-n* diodes as well as charge-coupled devices.

I. INTRODUCTION

Recent developments in controlled thermonuclear-fusion research require detailed analyses of plasma-electron behavior temporally and spatially. For this purpose, an x-ray tomographic-reconstruction technique[1–6] is employed as one of standard plasma-diagnostic methods in various types of plasma-confinement devices.[1–13] In particular, silicon surface-barrier (SSB) detectors have been widely used,[8–14] since they are easily handled and commercially available with a low cost.

However, a serious and important problem was recently found on the x-ray energy response; that is, a conventional and standard method of analyzing SSB data using the thickness of the depletion layer alone is not valid under current-mode operational conditions.[13,14] Data using two x rays at 8 and 17.5 keV have suggested that a possibility of the x-ray-sensitive region is not a depletion layer but a silicon-wafer thickness.[13] In fact, SSB wafer thicknesses were employed as x-ray-sensitive regions for analyzing x rays from tokamak plasmas.[13] If the wafer is essential to x-ray sensitivity, then we can easily design hard-x-ray detectors using thick silicon substrates, which are easily manufactured. This is quite attractive; however, after the publication of these papers, further research on the x-ray energy response of SSB detectors has not been made, and this mysterious but quite important problem for precise analyses of SSB data on x-ray radiation has not been solved even at this time. Furthermore, this strange and ambiguous property of the SSB detectors seems to discourage the use of SSB detectors for precise analyses of plasma-electron physics because of the lack of the analytical principle of SSB data.

In this paper, we propose a new theoretical model, which may correct the misunderstanding of the x-ray response characteristics of SSB detectors.

Our theoretical model, motivated by these important results,[13,14] may be extended to various types of solid-state detectors; for instance, charge-coupled devices (CCD)[15–18] and a multichannel array of silicon detectors (e.g., a linear image sensor[19]). Also, another purpose of this paper is to address this confusing situation and to generalize a systematic understanding of such solid-state detector responses.

An essential physical mechanism of our treatment adding to the conventional theory using the depletion layer is based on the inclusion of the thermal-diffusion effect of the charge that is created by incident x rays penetrating through the depletion layer and being absorbed in the silicon-substrate region. This diffusion effect may become a dominant term particularly for the 10 keV range x rays for widely used SSB detectors with a depletion-layer thickness of a few hundred μm. This effect enhances the x-ray sensitivity of SSB detectors in this high-energy x-ray range as compared with the conventionally estimated x-ray sensitivity using the depletion-layer thickness alone. Consequently, the contents and the physical interpretations in most of the previously reported research using x-ray data with SSB detectors (as well as *p-i-n* diodes in underbiased operations) should be carefully checked again and modified particularly for the discussions from data on such high-energy x rays. On the other hand, in a lower-energy region, the validity of the usage of the depletion-layer thickness alone is consistently confirmed even by this new theory; in this energy range, appreciable x-ray transmission through the depletion layer does not occur. In fact, the x-ray response data using synchrotron radiation in the

[a]Permanent address: Graduate School of Science and Technology, Niigata University, Niigata, Japan.
[b]Permanent address: Japan Atomic Energy Research Institute, Naka Fusion Research Establishment, Ibaraki, Japan.
[c]Permanent address: Semiconductor Division, Toshiba Microelectronics Center, Kawasaki, Japan.

 0021-8979/92/203363-11$04.00

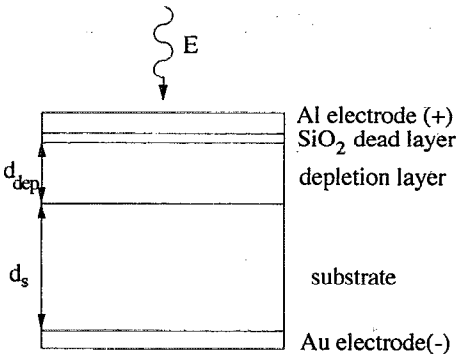

FIG. 1. Schematic structure of a partially depleted silicon surface-barrier (SSB) detector. A p^+-type silicon with an aluminum entrance window (an electrode) is employed. Note that there exist no electric field in the substrate and a strong electric field in the vertical direction of the depletion layer.

0.06–0.9 keV energy region[20] have been fitted by the theory, although some quantum effects including an x-ray-absorption near-edge structure (XANES) make a small deviation from the calculated result.

Furthermore, the validity of our theoretical analyses of the x-ray response of SSB detectors has been demonstrated by the 5–20 keV x-ray data using synchrotron radiation from a storage ring at the Photon Factory of the National Institute of High Energy Physics;[21] in this experiment, we have employed similar techniques when calibrating a microchannel plate as an x-ray detector.[22–25]

In this paper, we describe our theoretical model for the x-ray sensitivity of SSB detectors in detail. A forthcoming paper will be prepared for presenting both our experimental data and a comparison between this theory and the data.[21]

II. A THEORETICAL MODEL

Our theoretical model of the x-ray responses of SSB detectors is developed under a configuration of a widely used detector structure for plasma x-ray diagnostics (Fig. 1). Such a configuration is supplied as an R series fabricated by EG&G Ortec[26] and Tennelec,[27] etc.; the R series detectors are prepared for avoiding a response to visible light by using a light-proof aluminum electrode on the detector surface. A rear-side gold electrode with an ohmic contact is negatively biased; therefore, electrons created by incident photons drift to the grounded aluminum electrode. A thin silicon-dioxide dead layer ($\sim$100 Å) beneath the aluminum electrode partially attenuates the incident photons; attenuation of photons occurs in the electrode as well.

A voltage applied to the electrodes creates a depletion layer; charge created by incident photons in the depletion layer is quickly swept along a strong electric field produced by the applied voltage. The conventional and standard model is constructed under the above-described scheme.

In this paper, the importance of charge created by the x ray in the silicon substrate (p^+-type silicon for the R series) below the depletion layer is introduced in addition to the above conventional scheme; this field-free region essentially contributes to the high-energy x-ray response of SSB detectors as seen below. Charge created in the substrate does not experience an electric field but drifts slowly by a thermal-diffusion process. A fraction of the charge is recombined with impurity ions through the diffusion process. A direct recombination probability between an electron and a hole created is negligibly small. Charge reaching the depletion-layer boundary (at the bottom surface of the depletion layer in Fig. 1) is then detected as a signal at the aluminum electrode after drifting through the depletion layer. The charge-diffusion length L, which is comparable to the e-folding length of the charge population due to the charge recombination, is estimated from the relation of $L^2=D\tau$. Here, D and τ are a diffusion coefficient and the lifetime of the charge, respectively. The Einstein relation provides the equation of $D=\mu kT/e$; here, μ, k, T, and e are the mobility of the charge, the Boltzmann constant, a detector temperature in K, and the electronic charge, respectively. For minority carriers (electrons) in p-type silicon, μ is around $1.3\text{–}1.5\times10^3$ cm^2 (V s)$^{-1}$ at 300 K with an impurity doping of 10^{15}–10^{13} cm^{-3}. These values lead to the constant D of 34–39 cm^2 s^{-1}. The value of L is then estimated to be 75 μm with τ of 1.7–1.4 μs (see Refs. 15–17). These are reasonable values for standard silicon-semiconductor devices.

This estimation of L provides an important physical picture of the diffusion effect in the x-ray responses of SSB detectors; that is, an essential length of the charge-diffusion process in a substrate for SSB signal ranges of 50–100 μm.[15–17] This predicts that the thickness of a silicon wafer itself is unfortunately not essential to the SSB signal, since the charge created deeply in the substrate is recombined before reaching a depletion layer or an electrode. This property is also convenient to the calculation of the SSB response, since the cylindrical-boundary effect of the detector with a radius a of about 1 cm (for instance, a boundary-reflection effect of the charge) is negligible as compared with the total amount of directly diffusing charge from the substrate to the depletion layer.

Under these physical pictures, the following calculations of charge collection from both of the depletion layer and the substrate have been carried out.

A. A one-dimensional charge-diffusion model

In this subsection, we treat one-dimensional analyses of a charge-diffusion process in a silicon substrate. In general, one-dimensional methods are often employed because of their simplicity; whereas, the actual situation requires three-dimensional analyses because of the homogeneity of the charge-diffusion direction in the substrate. Nevertheless, the one-dimensional treatment (see Fig. 2) is convenient to make a rough estimation for the diffusion effect. In Sec. II B, we solve a three-dimensional diffusion equation, and then each result is compared for constructing a physical picture of the diffusion effect (see Sec. III).

A generalized diffusion equation is written as

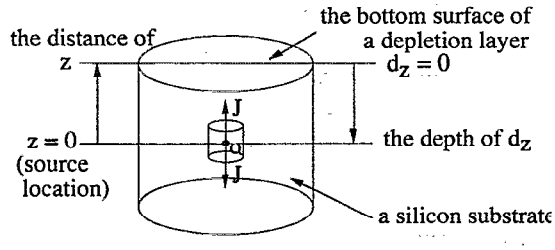

FIG. 2. Schematic view of the one-dimensional model for analyzing a charge-diffusion process in the substrate. The upper surface of the substrate is connected with the bottom surface of the depletion layer. X rays absorbed at the point 0 ($z=0$) create charge, and then the charge diffuses along the z axis (one-dimensional model). The source point $z=0$ exists at the depth d_z from the bottom surface of the depletion layer (or from the upper surface of the substrate). Note that the diffusion distance from $z=0$ to this surface equals d_z or z.

$$\mathrm{div}(D\ \mathrm{grad}\ \phi)-\Sigma\phi+s=\frac{\partial n}{\partial t}, \tag{1}$$

where ϕ is a "charge flux" described as nv, n and v are the density and the velocity of charge created in a substrate by x rays, respectively, and Σ is the charge-recombination coefficient (see below). The source charge s is created by incident x rays, and hence s is explicitly written per a unit time and a unit volume by using the incident x-ray intensity, its absorption rate in the substrate, and the charge-creation probability due to the x-ray absorption (see below).

In our case, the substrate is uniform; therefore, the first term on the left-hand side of Eq. (1) is written as

$$D\ \mathrm{div}\ \mathrm{grad}\ \phi=D\nabla^2\phi, \tag{2}$$

where ∇^2 is the Laplacian, and D is the diffusion coefficient of the charge.

As we estimate earlier, the recombination time τ ranges a few μs. Also, the temporal behavior of x-ray radiation from our plasmas varies slowly on the order of several ms. Therefore, the time scale of the diffusion process is sufficiently short compared with the temporal variation of the source x rays, which produce a "charge flux" ϕ in the substrate. Under this situation, the term including a time derivative is ignored; that is, a quasisteady state for the charge-diffusion process is treated as described above. This situation is valid for quasisteady current-mode operations of SSB detectors, particularly with the use of an integrator with a time constant of more than a few tens of μs; this is again guaranteed by the slowly varying plasma x-ray emission with time. (In a pulse-height analysis mode, the shaping time should be shorter than the diffusion time if one wants to escape from this diffusion effect. This is valid even for analyzing charged-particle energy analyses when they transmit a depletion layer.)

In this case, Eq. (1) is simplified as

$$D\nabla^2\phi-\Sigma\phi+s=0. \tag{3}$$

This is a steady-state diffusion equation or the Helmholtz equation.

The above generalized treatment is rewritten by using familiar parameters for the analyses of SSB-detector signals as follows:

$$\nabla^2 n-\frac{\Sigma}{D}n=\frac{1}{D}I_0\left(\frac{E}{\epsilon}\right)\mu\rho\exp(-\mu\rho d_z), \tag{4}$$

where n is again the charge density in the diffusion region; an x-ray flux I_0 with an energy E is incident to the upper surface of the diffusion region and then decreases to $I_0\exp(-\mu\rho d_z)$ at the depth of d_z from the surface. The value of ϵ stands for the energy required to create an electron-hole pair. The values of μ and ρ denote the silicon mass-absorption coefficient and the mass density, respectively. The minority-carrier diffusion length L is written as the square root of the ratio of D to Σ in the substrate; i.e., $L^2=D/\Sigma$.

Under the assumption of the one-dimensional approximation, the continuity equation (1) is written as

$$\frac{d^2\phi}{dz^2}-\frac{\phi}{L^2}=\frac{1}{D}I_0\left(\frac{E}{\epsilon}\right)\mu\rho\exp(-\mu\rho d_z). \tag{5}$$

To solve Eq. (5), it is useful to consider the physical picture of Eq. (5). The right-hand side of Eq. (5) denotes a source term at the location of created charge due to x-ray absorption; here, d_z denotes the depth from the bottom surface of the depletion layer to the source location 0 (see Fig. 2). To treat the diffusion of the created charge by using Eq. (5), the origin of the z axis ($z=0$) is introduced at the location of the x-ray-absorbed point for each absorption event. Therefore, the distance from the location of the source charge created by x rays to the lower surface of the depletion layer is written as $z=|d_z|$ as seen in Fig. 2. This length d_z or z is essential for the calculation of the diffusing charge from the source location to the lower surface of the depletion layer. The total x-ray absorption along the x-ray path in the z direction is, therefore, obtained by the integration over d_z or z, after the individual contribution of the charge created at the depth d_z and diffusing through the distance $z=|d_z|$ is solved [see below; in particular Eq. (13)]. This source term in Eq. (5) becomes zero except at the source position of $z=0$ for an x-ray-absorption event occurred at a "depth d_z" from the bottom surface of the depletion layer. From the viewpoint of the one-dimensional approximation, we can assume that charge diffusing from the source position $z=0$ flows only in the upward and the downward directions (Fig. 2). A fraction of the flow directed upward alone reaches the bottom surface of the depletion layer (its diffusion distance being $z=|d_z|$), and then is quickly swept to the aluminum electrode (much faster than the recombination time). Here, we define a flow density of the charge as $J(z)$, and we imagine a cylinder that encloses the source (Fig. 2). The relation between J and s is described as

$$\lim_{z\to 0}2\,J(z)=s=I_1\left(\frac{E}{\epsilon}\right)\mu\rho, \tag{6}$$

where I_1 denotes the x-ray intensity at a depth of d_z from the upper surface of the substrate (or the bottom surface of the depletion layer). This is the condition for the source.

At $z \neq 0$, Eq. (5) is written as

$$\frac{d^2\phi}{dz^2} - \frac{\phi}{L^2} = 0. \tag{7}$$

The solution of Eq. (7), which converges at $z \to \infty$, is obtained in the form of

$$\phi = A \exp(-z/L). \tag{8}$$

The relation between J and ϕ is written by using D as

$$J = -D\frac{d\phi}{dz}. \tag{9}$$

Thus, we obtain

$$J = \frac{DA}{L}\exp\left(\frac{-z}{L}\right) = \frac{s}{2}\exp\left(\frac{-z}{L}\right). \tag{10}$$

Here, it is noted again that a factor of $\frac{1}{2}$ comes from the one-dimensional flow in both of the upward and the downward directions.

The physical meaning of J is understood from a comparison between Eq. (9) and the first term of the left-hand side of Eq. (1); that is, the term div J gives a "leak rate" from the volume which includes the source. In other words, this term denotes the rate of charge diffusion from the volume, which is not recombined in the volume and is reached at the surface surrounding the volume. In our case, this volume corresponds to the region of the substrate and the surface is the bottom of the depletion layer. The other boundary of the substrate does not work as a charge-collection electrode or is sufficiently "far" as compared with the diffusion length. Furthermore, in the bottom region of the substrate, incident x rays themselves become weak because of their exponential attenuation due to the substrate; therefore, the charge reaching the rear electrode is negligible when we use a "thick" substrate as compared with a scale length of $(\mu\rho)^{-1}$.

This property is also confirmed by a volume integral of Eq. (1) as follows:

$$\frac{d}{dt}\int n\,dV = \int s\,dV - \int \Sigma\phi dV - \int \text{div}\,\mathbf{J}\,dV. \tag{11}$$

Each term on the right-hand side of Eq. (11) denotes a source rate in the volume V, a recombination rate in V, and a "leak" rate from the volume V, respectively, since the third term is replaced by $\int \mathbf{J}\,d\mathbf{S}$ where S is the surface surrounding the volume V. Consequently, in a quasisteady state, the "leak" rate of the charge reaching the surface S is described as a subtraction between the source term and the recombination term. From the above consideration, we focus our interest on the calculation of J for estimating the diffusion effect.

Equation (10) may be read that a source-charge s created at a depth d_z diffuses and decreases with an e-folding length of L, and then the fraction of $(\frac{1}{2})\exp(-z/L)$ reaches the surface of the depletion layer from the depth d_z. Also, at d_z, incident x rays attenuate and the intensity I_1 becomes $I_0 \exp(-\mu\rho d_z)$. (For simplicity, the subscripts of μ and ρ for a silicon will be omitted hereafter.) Therefore, the charge diffusing to the depletion layer from the depth d_z with the distance of z ($z = |d_z|$; see again Fig. 2) is described as

$$J_z = \frac{s}{2}\exp\left(-\frac{z}{L}\right) = \frac{1}{2}I_0\left(\frac{E}{\epsilon}\right)\mu\rho\exp(-\mu\rho z)\exp\left(-\frac{z}{L}\right). \tag{12}$$

The integral over z from 0 to the thickness of the substrate d_s gives a total charge Q_D, which diffuses from the substrate to the bottom surface of the depletion layer, and results in a part of the SSB output signal,

$$\begin{aligned} Q_D &= \int_0^{d_s} \frac{s}{2}\exp\left(-\frac{z}{L}\right)dz \\ &= \frac{1}{2}I_0\left(\frac{E}{\epsilon}\right)\mu\rho\int_0^{d_s}\exp\left[-\left(\mu\rho+\frac{1}{L}\right)z\right]dz \\ &= \frac{1}{2}I_0\left(\frac{E}{\epsilon}\right)\frac{\mu\rho}{\mu\rho+1/L}\left\{1-\exp\left[-\left(\mu\rho+\frac{1}{L}\right)d_s\right]\right\}, \end{aligned} \tag{13}$$

where Q_D stands for the sum of the diffusing charge fraction reaching the depletion layer; here, the charge is created along the x-ray path. In the case of a thick substrate [i.e., $L \ll d_s$ and $(\mu\rho)^{-1} \ll d_s$], Eq. (13) is then approximately rewritten as

$$Q_D \approx \frac{1}{2}I_0\left(\frac{E}{\epsilon}\right)\frac{\mu\rho L}{\mu\rho L+1}. \tag{14}$$

On the other hand, the contribution of charge created in the depletion layer Q_{dep} is written as

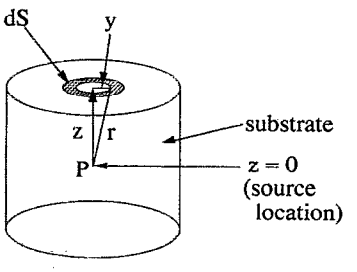

FIG. 3. Schematic view of the three-dimensional model for the charge-diffusion process in the substrate. The upper surface corresponds to the bottom surface of the depletion layer. Charge diffusing from the source (point P) to the depletion layer is calculated.

$$Q_{\mathrm{dep}}=I_{\mathrm{dep}}\left(\frac{E}{\epsilon}\right)\int_0^{d_{\mathrm{dep}}}\mu\rho\exp(-\mu\rho z)dz$$
$$=I_{\mathrm{dep}}\left(\frac{E}{\epsilon}\right)[1-\exp(-\mu\rho d_{\mathrm{dep}})], \tag{15}$$

where the thickness of the depletion layer is denoted by d_{dep}, and the incident x-ray intensity into the upper surface of the depletion layer I_{dep} is related to I_0 as

$$I_0=I_{\mathrm{dep}}\exp(-\mu\rho d_{\mathrm{dep}}). \tag{16}$$

Using Eqs. (14) and (15), a total charge Q_t obtained with the SSB detector due to an x-ray intensity from plasmas I_{plas} is written as

$$Q_t=Q_{\mathrm{dep}}+Q_D=I_{\mathrm{dep}}\left(\frac{E}{\epsilon}\right)\left\{[1-\exp(-\mu\rho d_{\mathrm{dep}})]+\frac{1}{2}\exp(-\mu\rho d_{\mathrm{dep}})\frac{\mu\rho L}{\mu\rho L+1}\right\}$$
$$=I_{\mathrm{plas}}\exp(-\mu_{\mathrm{SiO_2}}\rho_{\mathrm{SiO_2}}d_{\mathrm{dead}})\exp(-\mu_{\mathrm{Al}}\rho_{\mathrm{Al}}d_{\mathrm{elect}})\left(\frac{E}{\epsilon}\right)\left(1-\exp(-\mu\rho d_{\mathrm{dep}})+\frac{1}{2}\exp(-\mu\rho d_{\mathrm{dep}})\frac{\mu\rho L}{\mu\rho L+1}\right). \tag{17}$$

where the subscripts dead and elect denote the dead layer and the electrode, respectively (see Fig. 1).

In previous papers on CCD detectors,[15–17] a similar formula to Eq. (17) was reported as x-ray response except for a factor of $\frac{1}{2}$ on the right-hand side of Eq. (17). This is quite reasonable since these CCD papers assume upward diffusion alone for the response calculation. The result of Eq. (17) is modified in the following subsection so as to include a three-dimensional effect; however, such similar responses in SSB and CCD detectors suggest a possibility of a widely existing physics principle in these solid-state detectors. In turn, such a finding of general physics principles may suggest possibilities of the developments of various designs of new-type detectors.

B. A three-dimensional charge-diffusion model

In this section, a three-dimensional charge-diffusion equation is solved for evaluating SSB detection characteristics under a rather reliable situation as compared with the assumption for the simplified one-dimensional analysis treated in Sec. II A. An essential difference of the physical picture for the three-dimensional treatment is charge diffusion allowed in every direction; therefore, we introduce a three-dimensional diffusion equation (18) (see below) for charge created in the substrate in place of Eq. (5). For the physical picture of the charge-collection process, similar treatments explained in the one-dimensional treatment in Sec. II A are valid except the diffusion direction; this makes it possible to absorb ourselves in solving a rather complicated Eq. (18) under our physical understanding constructed in Sec. II A. The three-dimensional diffusion equation is written as

$$\frac{1}{r^2}\frac{d}{dr}r^2\frac{d\phi(r)}{dr}-\frac{1}{L^2}\phi(r)=-\frac{s(d)}{D}. \tag{18}$$

This equation is solved using a similar method treated in Sec. II A. At any location except the source position, Eq. (18) is described as

$$\frac{1}{r^2}\frac{d}{dr}r^2\frac{d\phi(r)}{dr}-\frac{1}{L^2}\phi(r)=0. \tag{19}$$

The relation between J and s is given by

$$\lim_{r\to 0}4\pi r^2J(r)=s. \tag{20}$$

Here, we imagine a sphere with a radius r surrounding the location of the source $s(r=0)$ in place of the cylinder (Fig. 2) used for solving Eq. (6). Thus, $J(r)$ is described as

$$J=-D\frac{d\phi}{dr}=\frac{s}{4\pi r^2}\left(\frac{r}{L}+1\right)\exp\left(-\frac{r}{L}\right), \tag{21}$$

where

$$s=I_1\left(\frac{E}{\epsilon}\right)\mu\rho. \tag{22}$$

At a depth of d from the upper surface of the substrate, I_1 is related to I_0 as

$$I_1=I_0\exp(-\mu\rho d). \tag{23}$$

As noted in the one-dimensional treatment, d may be replaced by z for the x-ray incidence along the z axis. Charge created at this point P (Fig. 3) diffuses in every direction. As described in Sec. II A, charge reaching the bottom surface of the depletion layer contributes to a SSB signal. Therefore, we at first calculate the total charge $R(z)$ from the point P to the depletion-layer surface. Here, it is convenient to use the relation of $r^2=y^2+z^2$ (see Fig. 3). Charge diffusing from P to an area dS with a radius of y and a width of dy (Fig. 3) is then defined as $dR(y)$, and is written by $dR(y)=2\pi yJ(r)dy$.

The total charge $R(z)$ is now obtained by

$$R(z)=\int_{y=0}^{a} 2\pi y J(r)\,dy$$
$$=\int_{r=z}^{\sqrt{z^2+a^2}} 2\pi\,\frac{s}{4\pi r^2}\left(\frac{r}{L}+1\right)\exp\left(-\frac{r}{L}\right)r\,dr$$
$$=\frac{1}{2}I_0\left(\frac{E}{\epsilon}\right)\mu\rho\exp(-\mu\rho z)$$
$$\times\int_{r=z}^{\sqrt{z^2+a^2}}\left(\frac{1}{L}+\frac{1}{r}\right)\exp\left(-\frac{r}{L}\right)dr. \tag{24}$$

As we discussed in Sec. II A, most of the charge diffusing from the substrate region comes within a length of a few times L below the depletion layer. The radius a is much larger than L; therefore, Eq. (24) is approximately written as

$$R(z)=\frac{1}{2}I_0\left(\frac{E}{\epsilon}\right)\mu\rho\exp(-\mu\rho z)\left[\exp\left(-\frac{z}{L}\right)+\int_{r=z}^{a}\frac{1}{r}\exp\left(-\frac{r}{L}\right)dr\right]$$
$$\approx\frac{1}{2}I_0\left(\frac{E}{\epsilon}\right)\mu\rho\exp(-\mu\rho z)\left[\exp\left(-\frac{z}{L}\right)+E_1\left(\frac{z}{L}\right)\right], \tag{25}$$

where $E_1(x)$ is the exponential integral[28] and is defined by

$$E_1(x)=\int_x^{\infty}\frac{\exp(-t)}{t}\,dt. \tag{26}$$

In Eq. (25), we use the characteristics of $E_1(x)$; that is, $E_1(x)$ decreases quickly with increasing x.

We then integrate over z from 0 to the thickness of the substrate d_s; this integration W_0 corresponds to a scan of the source point P in the substrate along the x-ray path in the z direction,

$$W_0=\int_0^{d_s}R(z)\,dz. \tag{27}$$

It is again noted that under the condition of $L\ll a\sim 10$ mm cylindrical boundary effects are negligible; thus, this calculated result also represents a total response of the SSB detector for a unit intensity of well-collimated x-ray influx (a quasiparallel beam) even if the influx is incident on the whole detector surface.

The contribution of the first term on the right-hand side of Eq. (25) to W_0 is defined by W_1, and is described as

$$W_1=\frac{1}{2}I_0\left(\frac{E}{\epsilon}\right)\mu\rho\int_0^{d_s}\exp\left[-\left(\mu\rho+\frac{1}{L}\right)z\right]dz. \tag{28}$$

This is the same form as Eq. (13) from the one-dimensional treatment. Thus, at the limits of $L\ll d_s$ and $(\mu\rho)^{-1}\ll d_s$, W_1 then becomes

$$W_1\approx\frac{1}{2}I_0\left(\frac{E}{\epsilon}\right)\frac{\mu\rho L}{\mu\rho L+1}. \tag{29}$$

The second term on the right-hand side of Eq. (25) partially contributes to W_0, and is defined by W_2. This is described as

$$W_2=\frac{1}{2}I_0\left(\frac{E}{\epsilon}\right)\mu\rho\int_0^{d_s}\exp(-\mu\rho z)E_1\left(\frac{z}{L}\right)dz. \tag{30}$$

For our partially depleted SSB detector, an approximation of $d_s\to\infty$ is also utilized under the condition of $d_s\gg L$; in this case, the calculated result from Eq. (30) using the Laplace transform is

$$W_2=\tfrac{1}{2}I_0(E/\epsilon)\ln(1+\mu\rho L). \tag{31}$$

Thus, the total charge diffusing from the substrate due to a unit x-ray influx I_0 onto a unit area of the bottom surface of the SSB depletion layer is described as

$$W_0\approx\frac{1}{2}I_0\left(\frac{E}{\epsilon}\right)\left(\frac{\mu\rho L}{\mu\rho L+1}+\ln(1+\mu\rho L)\right). \tag{32}$$

The contribution from the depletion layer is the same form as Eq. (15). Therefore, using Eqs. (15) and (32) the totally collected charge Q_T created in both a depletion layer and a sufficiently thick substrate is described as

$$Q_T=I_{\rm plas}\exp(-\mu_{\rm SiO_2}\rho_{\rm SiO_2}d_{\rm dead})\exp(-\mu_{\rm Al}\rho_{\rm Al}d_{\rm elect})\left(\frac{E}{\epsilon}\right)$$
$$\times\left[1-\exp(-\mu\rho d_{\rm dep})+\frac{1}{2}\exp(-\mu\rho d_{\rm dep})\left(\frac{\mu\rho L}{\mu\rho L+1}+\ln(1+\mu\rho L)\right)\right], \tag{33}$$

where the three-dimensional treatment for the diffusion effect is utilized.

For the derivation of Eq. (32), we assume the relation of $a\gg L$ to avoid mathematical complexity. In actual experiments, this relation is easily satisfied when we use a collimator with a radius of less than $a-c$ placed just in front of a SSB surface (the length of c being a few times larger than L). When we explicitly express the terms including a, we then merely add the following terms to the value of W_0 in Eq. (32); that is,

$$\frac{1}{2}I_0\left(\frac{E}{\epsilon}\right)\left(-\mu\rho\left(\frac{\pi La}{2}\right)^{1/2}\left[\operatorname{erfc}\left[\mu\rho\left(\frac{La}{2}\right)^{1/2}\right]-\operatorname{erfc}\left(\frac{d_s+L\mu\rho a}{\sqrt{2La}}\right)\right]\exp\left(\frac{a}{2L}(L^2\mu^2\rho^2-2)\right)-E_1\left(\frac{a}{L}\right)\right), \tag{34}$$

where

$$\operatorname{erfc}(z)=1-\operatorname{erf}(z)=1-\frac{2}{\sqrt{\pi}}\int_0^z\exp(-t^2)\,dt. \tag{35}$$

Here, the terms including the error function come from the integral of

$$I_0\frac{E}{2\epsilon}\int_0^{d_s}\exp\left[-\left(\mu\rho z+\frac{\sqrt{z^2+a^2}}{L}\right)\right]dz,$$

[see Eq. (24) with the assumption of $L \sim z \ll a$].

In place of the relation of $d_s \gg L$, even if d_s merely satisfies the relation of $d_s > L$, then the dependence of charge diffusion, $r^{-1}\exp(-r/L)$, guarantees a remarkable diffusion contribution represented by Eq. (32). This is also found in Eq. (25); that is, for the values of $E_1(z/L)$, the ratio of $E_1(2L/L)$ to $E_1(0.5L/L)$ is merely about 0.087. From this fact, in the region of $z \gg 2L$ the contribution of the diffusion effect is quite small. [Also, note that the second term including $E_1(z/L)$ in Eq. (25) is always larger than the first term in Eq. (25).] This characteristic of a short-length contribution of the diffusion is analogous to quickly decreasing nuclear force with increasing the distance; this nuclear force is written by the well-known Yukawa potential equation,[29] which is the same form as our equation.

Furthermore, for SSB detectors with $d_s \approx L$, a fraction of the diffusion effect becomes somewhat smaller as compared with the above-calculated result; in this case, one may easily carry out the calculations of the diffusion amount according to the same integrals although the upper integral limits are changed. The characteristics of these SSB detectors resemble the responses of *p-i-n* diodes in a fully biased operation or in a completely depleted diode operation; under such operating conditions, there exists no field-free substrate region; however, it is noted that even for the use of *p-i-n* diodes, the diffusion effect should be taken into account in an underbiased operation. Furthermore, the diffusion effect is enhanced for SSB detectors when one uses them in an underbiased operation, since a depletion-layer thickness is proportional to the square root of an applied bias and then the thickness of a field-free substrate region increases.

III. CALCULATED RESULTS AND DISCUSSION

Numerically calculated results using the three-dimensional theoretical model described in Sec. II are shown in this section, and thereby the importance of the charge-diffusion effect in the substrate region is demonstrated. The comparison between this new model and the conventional model of charge collection from a depletion layer alone is then made.

The solid curves in Fig. 4 show numerical results using Eq. (33) with $d_{\text{dep}}=218$ μm and various values of L; namely, $L=0$, 25, 50, 75, 100, and 125 μm. The lowest curve in Fig. 4 corresponds to $L=0$; this curve has commonly been utilized for the SSB response in most plasma x-ray papers published previously. The value of d_{dep} was supplied by an SSB manufacturer.[27] The accuracy of the data supplied was, for instance, confirmed experimentally by using pulse-height analyses.[30] The SSB parameters described above are chosen for the calibration experiments of a SSB detector using synchrotron radiation. (The preliminary results which support our new theoretical model are reported in Ref. 21.) Here, we chose an SSB detector with a thick wafer of 360 μm so as to satisfy the relation of $d_s > L$. The x-ray response using this wafer thickness as a depletion layer[13] is also shown by the top trace (dashed curve) in Fig. 4. As we described, the value of L for our

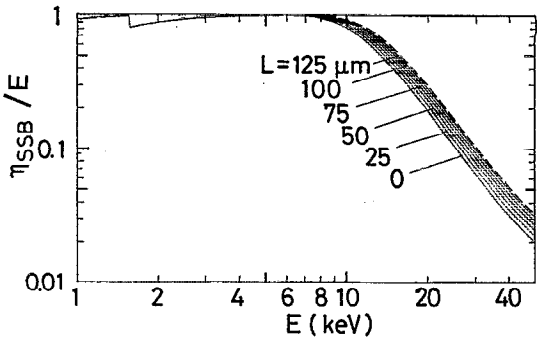

FIG. 4. X-ray energy response of a SSB detector η_{SSB} [$=Q_T/I_{\text{plas}}$; see Eq. (33)]. The following parameters of our SSB detector [utilized in our calibration experiments (see Ref. 21)] are substituted into Eq. (33) for obtaining the totally collected charge Q_T created by the x-ray flux from plasmas I_{plas}; the depletion-layer thickness of 218 μm, and the diffusion length L of 75 μm. For comparison, the results from $L=0$ (charge collection in the depletion layer alone), 25, 50, 100, and 125 μm are depicted by the solid curves. Also, the wafer thickness of 360 μm is assumed as an x-ray-sensitive layer thickness for the dashed curve.

SSB detector is estimated to be 75 μm.[15–17] Therefore, three SSB-response models using (i) a depletion-layer thickness alone, (ii) a total wafer thickness as a depletion layer,[13] and (iii) our new treatment based on a combination of a depletion-layer thickness and a diffusion length may be compared and evaluated by fitting experimental calibration data[21] to the theoretical curves (Fig. 4).

Next, we compare the results from the one-dimensional approximation in Sec. II A with those from the three-dimensional calculations in Sec. II B. The three-dimensional effect is particularly characterized by an additional term including $\ln(1+\mu\rho L)$ [see Eqs. (32) and (33)]. It is again noted that this term originated from the integral of

$$\frac{1}{2} I_0 \frac{E}{\epsilon} \mu\rho \int_{z=0}^{d_s} \exp(-\mu\rho z) \left[\int_{r=z}^{\sqrt{z^2+a^2}} \frac{1}{r} \exp\left(-\frac{r}{L}\right) dr \right] dz.$$

This means that the essential contribution from the three-dimensional integral added to the result from the one-dimensional effect comes from the second term of J expressed in Eq. (21).

On the other hand, an identical contribution from either one- or three-dimensional treatment is originated from the following integral calculations. For the one-dimensional case, this integral is

$$\int_{z=0}^{d_s} J_z \, dz = \int_{z=0}^{d_s} \frac{1}{2} s \exp\left(-\frac{z}{L}\right) dz = \frac{1}{2} I_0 \frac{E}{\epsilon} \mu\rho \int_{z=0}^{d_s} \exp(-\mu\rho z) \exp\left(-\frac{z}{L}\right) dz. \tag{36}$$

On the other hand, for the three-dimensional model, the first term of J in Eq. (21) results in the same value as the integral of Eq. (36) [see Eqs. (28) and (29)], while the second term in Eq. (21) provides the following three-dimensional contribution [see Eq. (31)]:

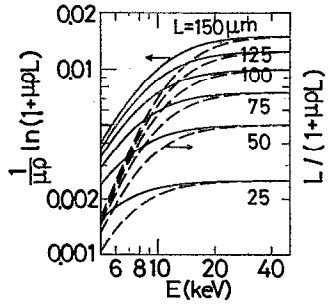

FIG. 5. The comparison of the terms of $\ln(1+\mu\rho L)$ and $\mu\rho L/(\mu\rho L+1)$ with $L=25$ (the lowest trace), 50, 75, 100, 125, and 150 μm (the top trace); these two terms are normalized by $\mu\rho$. The solid and dashed curves correspond to each term, respectively. The latter term characterizes the one-dimensional treatment, while the sum of both terms results from the three-dimensional treatment [see Eq. (32) for the three-dimensional diffusion model, and Eq. (14) for the one-dimensional diffusion model].

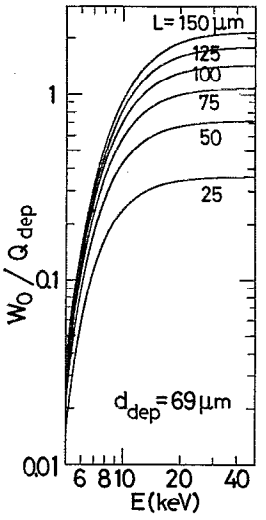

FIG. 6. The signal contribution ratio of the charge-diffusion effect W_0 from the substrate [Eq. (32)] to the collected charge created in the depletion layer Q_{dep} [Eq. (15)]. Parameters of the depletion-layer thickness of 69 μm and $L=25$ (the lowest trace), 50, 75, 100, 125, and 150 μm (the top trace) are used. Note that this ratio becomes more than unity for high-energy x rays when L becomes longer than 69 μm; that is, the diffusion becomes predominant for a SSB signal.

$$\int_{r=z}^{\sqrt{z^2+a^2}} \frac{s}{4\pi r^2}\left[\frac{r}{L}\exp\left(-\frac{r}{L}\right)\right]2\pi r\,dr$$
$$=\frac{1}{2}I_0\frac{E}{\epsilon}\mu\rho\int_{z=0}^{d_s}\exp(-\mu\rho z)$$
$$\times\left[\int_{r=z}^{\sqrt{z^2+a^2}}\frac{1}{r}\exp\left(-\frac{r}{L}\right)dr\right]dz. \quad (37)$$

These integrals of Eqs. (36) and (37), which are characterized by $\mu\rho L/(1+\mu\rho L)$ and $\ln(1+\mu\rho L)$, respectively, are numerically compared in Fig. 5, where these two values are normalized by $\mu\rho$. A larger contribution of the integrated result including $\ln(1+\mu\rho L)$ is found in Fig. 5 particularly for $h\nu<10$ keV; this tendency is remarkable for the curves with larger values of L. It is also noted that for x rays in the energy range of a few tens of keV the contribution from each term becomes comparable. This is easily understood using the relation of $\mu\rho L\ll 1$ for this high-energy x-ray region. At this limit, each term approaches the same value of $\mu\rho L$. (In Fig. 5, the values in the ordinate are normalized by $\mu\rho$; thereby, the curves approach their corresponding values of L in units of cm.)

Furthermore, this dependence on L for SSB signals indicates an intensive contribution from a substrate with a larger value of L. This feature is seen in Fig. 5 and is understood as follows: For a substrate with a smaller value of L, high-energy x rays penetrate the substrate deeply and are absorbed there, where the penetration length is characterized by $(\mu\rho)^{-1}$. These x rays do not contribute to the output signals of SSB detectors, since the diffusing charge in the substrate is recombined within a short distance of the order of L (see Sec. II B), and then the location of the created charge reaching a depletion layer is restricted within a shallow region from the depletion layer. This unfortunately makes it impossible to realize the expectation of the validity of a silicon-wafer thickness as an x-ray-sensitive layer.[13]

This characteristic feature depending on the length L may give technical information on the design of partially depleted SSB detectors with high sensitivity; these detectors are required to have a long range of L. For satisfying this requirement, a doping rate of impurities as recombination centers should be minimized; this automatically means the necessity of a thicker wafer as compared with this length of L. However, it is noted that this requirement is necessary only for the use of the partially depleted SSB detectors in a current-mode operation, since the charge-collection time becomes longer with increasing L. Thus, in a pulse-height analysis operation, L should be limited within a corresponding length to a charge-collection time of L/v as compared with a shaping time for the pulse-height analyses, where v is the thermal-diffusion velocity of minority charge in a substrate. For this purpose, the optimization of doping impurities might be necessary.

Also, it is important to note that collected charge contributing to a SSB signal and originated from a depletion layer is written as $1-\exp(-\mu\rho d_{dep})$ for a unit x-ray influx; in the cases with $\mu\rho d_{dep}\ll 1$, the collected charge is approximately described as $\mu\rho d_{dep}$. This provides similar behavior to the diffusion in the above-discussed limiting case with $\mu\rho L\ll 1$. Under these two limiting conditions of $\mu\rho L\ll 1$ (i.e., for high-energy x rays) and $\mu\rho d_{dep}\ll 1$ the same contributions to a SSB signal from the substrate and the depletion layer are expected in the case with $d_{dep}\approx L$.

In the case with $d_{dep}\ll L$, a contribution from the charge-diffusion effect in a substrate becomes dominant for a SSB signal (Fig. 6); in this case, the effect of the variation of a depletion-layer thickness depending on the supplied bias to the SSB detector may be masked by a predominant effect of the diffusion.

Figure 5 also evaluates the calculated results from the one-dimensional approximation (the dashed curve) as

compared with those from the three-dimensional treatment (the sum of the values of the dashed and solid curves). A previously published model for a CCD detector response might become a reference for the one-dimensional approximation.[15–17] However, in these papers, a factor of $\frac{1}{2}$ in Eq. (14) is lacking; this originates from the assumption of charge diffusion in the upward direction alone. As long as the approximation of $\mu\rho L/(1+\mu\rho L)\approx\ln(1+\mu\rho L)$ is satisfied under the condition of $\mu\rho L\ll 1$, this simplified one-dimensional model happens to provide suitable results; that is, in actual experiments, the lack of a factor of $\frac{1}{2}$ from this simplified model is incidentally compensated by the three-dimensional effect evaluated from the term of $\ln(1+\mu\rho L)$ as depicted by the solid curve in Fig. 5 [see Eq. (37)]. As we discussed above, this result is satisfied only in the higher x-ray energy region (see again the overlap region of the solid and the dashed curves in Fig. 5). However, the physical picture of each diffusion process (in particular, for the diffusion direction) is essentially different in each treatment even though both of the previous model[15–17] and our new model in Sec. II A are based on one-dimensional treatments. The three-dimensional effect discribed in both Eqs. (36) and (37) as well as the property of $\mu\rho L/(1+\mu\rho L)\approx\ln(1+\mu\rho L)$ happens to provide a good agreement between the result from our three-dimensional model [i.e., the sum of Eqs. (36) and (37)] and the result from the previous one-dimensional model with a single-directional diffusion [i.e., the integral in Eq. (36) alone, but a factor of 2 being fortunately multiplied in the previous papers notwithstanding the use of the assumption of the single-directional flow].[15–17] Note again that the factor of $\frac{1}{2}$ in our one-dimensional treatment comes from the complete minority-charge recombination for the downward-diffusing charge.

The difference between the previous one-dimensional approximation (see the dashed curves in Fig. 5 with the multiplication of a factor of 2) and our three-dimensional treatment (see the sum of the values of the solid and the dashed curves in Fig. 5) becomes larger in the lower-energy regions.

However, it is again fortunate that the contribution of the charge diffusing from a substrate becomes relatively smaller than the contribution of the charge created in the depletion layer due to x rays with such lower energies. Therefore, although the previous one-dimensional approximation seems to become worse for these low-energy x rays, the total detector response masked by the contribution of the charge created in the depletion layer tends to be fitted by the calculated results using the simplified one-dimensional model.

Figure 7 shows the contributed fraction of diffusing charge from a substrate W_0 [Eq. (32)] to collected charge created in the depletion layer $Q_{\rm dep}$ [Eq. (15)]; here, the parameters in Fig. 4 are employed. It is reasonable that an appreciable contribution of the diffusion starts from the energy beyond which the x-ray penetration through the depletion layer into the substrate begins to be remarkable. This critical energy may be found from the curve with $L=0$ in Fig. 4; the efficiency calculated from the use of the depletion-layer thickness alone starts to decrease beyond this energy because of the penetration of x rays.

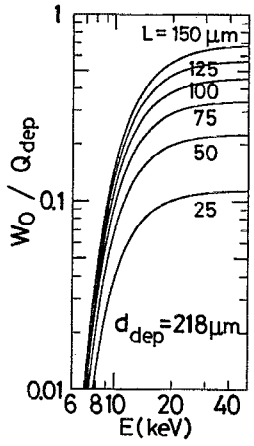

FIG. 7. The signal-contribution ratio of the charge-diffusion effect W_0 from the substrate to the collected charge created in the depletion layer $Q_{\rm dep}$. The parameters of a 218-μm-thick depletion layer used in Fig. 4 and the same values of L in Fig. 6 are employed.

Also, the ratio of the diffusion effect increases with increasing L. This results from the increase of collected charge due to the reduction of a recombination rate. In Fig. 7, it is noted that this ratio becomes unity in the case of $d_{\rm dep}=L$.

The above-described method has been developed for analyzing SSB data in a current-mode operation. This method is essentially applicable to CCD data analyses. This treatment might provide an alternative analyzing method of evaluating the energy responses for image-sensor applications although recent theoretical papers on CCD analyses tend to be prepared for the analyses in a pulse-height analysis operation, for which time-derivative terms may not be ignored because of a finite time for charge collection limited by the shaping time. However, as noted earlier, when the shaping time is longer than a charge-diffusion time, the above compact formula may be widely available.

Finally, it might be better to note the physical picture described above; such a physical understanding of the charge-collection mechanism will give useful information on its future applications to three-dimensional imaging detectors as well as on a generalized understanding of semiconductor detectors, which might cover an essential common physics underlying SSB, CCD, and *p-i-n* diode detectors.

IV. SUMMARY

A new theoretical model for x-ray energy responses of partially depleted SSB detectors has been proposed in a current-mode operation. A commonly utilized method for SSB data analyses, which is based on a depletion-layer thickness alone as an x-ray sensitive layer, is found to be corrected although this method has widely been believed to be valid for x-ray analyses in various types of plasma-confinement devices for nuclear fusion research.

Our new model supporting the calibration data[21] is characterized by the inclusion of a charge-diffusion effect in a substrate region where no electric field exists. In our model, adding to this charge-diffusion effect, the collection of charge created in the depletion layer is also taken into account. A remarkable enhancement of the sensitivity for high-energy x rays is evaluated as compared with the result calculated from the conventional model using the depletion layer alone (compare the numerically calculated curves labeled with $L=0$ and with $L=75$ μm in Fig. 4 for finding a typical diffusion effect).

The physical picture of the diffusion effect is described as follows: Charge is created in a substrate by x rays penetrating through a depletion layer. Then, the charge created in the substrate thermally diffuses in every direction. The diffusing charge is partially recombined in the substrate, and consequently a fraction of the charge reaches the depletion layer. A strong electric field in the depletion layer quickly sweeps the charge to an electrode, and then this partially contributes to an SSB signal, adding to the conventional contribution of charge created in the depletion layer.

Mathematical analyses of the diffusion process are carried out using a one-dimensional diffusion equation for understanding a rather simplified physical background of our model; also, a three-dimensional charge-diffusion equation is analytically solved and a convenient formula of Eq. (33) is represented for the use of a SSB detector with a thicker substrate as compared with the diffusion length. Roughly speaking, the three-dimensional calculations indicate a larger diffusion contribution by a factor of about 2 as compared with the result from the one-dimensional treatment; this feature is seen in Fig. 5 as the dashed curve for the diffusion effect from the one-dimensional treatment and as a combination of the values of the dashed and solid curves for the diffusion evaluation from the three-dimensional model.

Such a diffusion effect becomes essentially of importance for partially depleted SSB detectors particularly in the use of underbiased operations, which are widely employed for plasma x-ray diagnostics in various devices. From our new model, the same situation is also expected for the use of *p-i-n* diodes in underbiased operations as well as CCD detectors in current-mode operations. These, in turn, suggest the existence of a generally underlying physical treatment covering over the energy responses of such semiconductor detectors; such a viewpoint might be quite useful for the application and the future development of these detectors.

ACKNOWLEDGMENTS

The authors would like to acknowledge useful discussions with Professor S. Tanaka of Kyoto University, Professor S. Aoki of University of Tsukuba, as well as Professor H. Maezawa and Dr. X. Zhang of the Photon Factory at National Laboratory for High Energy Physics. They also would like to acknowledge the members of the GAMMA 10 Group for their collaboration. Useful information on silicon detectors is given by H. Suzuki of Seiko Instruments Inc., S. Miyahara of Seiko EG&G Co. Ltd., M. Niki of Niki Glass Co. Ltd., Dr. C. Winsor and Dr. M. Martini of EG&G Ortec, and Dr. W. Richardson of Tennelec Inc. is greatly appreciated. Financial support of the work was partly provided by a Grant-in-Aid for Scientific Research from the Ministry of Education of Japan.

[1] A. M. Cormack, J. Appl. Phys. **34**, 2722 (1963); **35**, 2908 (1964).
[2] T. Cho, M. Hirata, K. Ogura, E. Takahashi, T. Kondoh, N. Yamaguchi, K. Masai, K. Hayashi, I. Katanuma, K. Ishii, T. Saito, Y. Kiwamoto, K. Yatsu, and S. Miyoshi, Phys. Rev. Lett. **64**, 1373 (1990).
[3] T. Cho, M. Hirata, E. Takahashi, K. Ogura, K. Masai, N. Yamaguchi, T. Kondoh, K. Matsuda, H. Hojo, M. Inutake, K. Ishii, Y. Kiwamoto, A. Mase, T. Saito, K. Yatsu, and S. Miyoshi, Phys. Rev. A **45**, 2532 (1992).
[4] T. Kondoh, T. Cho, M. Hirata, N. Yamaguchi, T. Saito, Y. Kiwamoto, and S. Miyoshi, J. Appl. Phys. **67**, 1694 (1990).
[5] Y. Nagayama, J. Appl. Phys. **62**, 2702 (1987).
[6] S. Tsuji, Y. Nagayama, K. Miyamoto, K. Kawahata, N. Noda, and S. Tanahashi, Nucl. Fusion **22**, 1082 (1982); **25**, 305 (1985).
[7] T. Cho, M. Inutake, K. Ishii, I. Katanuma, Y. Kiwamoto, A. Mase, Y. Nakashima, T. Saito, N. Yamaguchi, K. Yatsu, M. Hirata, T. Kondoh, H. Sugawara, J. H. Foote, and S. Miyoshi, Nucl. Fusion **28**, 2187 (1988).
[8] TFTR group, in *Proceedings of the Eleventh International Conference on Plasma Physics and Controlled Nuclear Fusion Research*, Kyoto, Japan, 1986, edited by J. W. Weil and M. Demir (IAEA, Vienna, 1987), Vol. I, p. 51; J. Kiraly, M. Bitter, P. Efthimion, S. Von Goeler, B. Grek, K. W. Hill, D. Johnson, K. McGuire, N. Sauthoff, S. Sesnic, F. Stauffer, G. Tait, and G. Taylor, Nucl. Fusion **27**, 397 (1987).
[9] T. Cho, K. Ogura, A. Ando, H. Tanaka, M. Nakamura, S. Nakao, T. Shimozuma, S. Kubo, T. Maekawa, Y. Terumichi, and S. Tanaka, Nucl. Fusion **26**, 349 (1986).
[10] T. Cho, T. Kondoh, M. Hirata, A. Sakasai, N. Yamaguchi, A. Mase, Y. Kiwamoto, A. Hirose, K. Ogura, S. Tanaka, and S. Miyoshi, Nucl. Fusion **27**, 1421 (1987).
[11] M. Hirata, T. Cho, E. Takahashi, K. Masai, K. Ogura, K. Koganezawa, N. Yamaguchi, T. Kato, T. Kondoh, K. Ishii, T. Saito, Y. Kiwamoto, K. Yatsu, and S. Miyoshi, Nucl. Fusion **31**, 752 (1991).
[12] K. Ogura, H. Tanaka, S. Ide, M. Iida, K. Hanada, M. Yoshida, T. Minami, T. Cho, M. Nakamura, T. Maekawa, Y. Terumichi, and S. Tanaka, Nucl. Fusion **31**, 1015 (1991).
[13] K. W. Wenzel and D. Petrasso, Rev. Sci. Instrum. **59**, 1380 (1988); **61**, 693 (1990); and references therein.
[14] X. Chen and R. D. Petrasso, Rev. Sci. Instrum. **61**, 2815 (1990).
[15] L. N. Koppel, in *Advances in X-Ray Analysis*, edited by R. W. Gould, C. S. Barrett, J. B. Newkirk, and C. O. Ruud (Plenum, New York, 1975), Vol. 19, p. 587.
[16] L. N. Koppel, Rev. Sci. Instrum. **48**, 669 (1977).
[17] M. C. Peckerar, W. D. Baker, and D. J. Nagel, J. Appl. Phys. **48**, 2565 (1977).
[18] H. Tsunemi, S. Kawai, and K. Hayashida, Jpn. J. Appl. Phys. **27**, 670 (1988); **30**, 1299 (1991).
[19] Seiko Instruments Inc., A linear image sensor catalogue; H. Suzuki, Seiko Instruments Inc., Takatsuka, Matsudo-shi 271, Japan (private communication).
[20] T. Cho, M. Hirata, E. Takahashi, N. Yamaguchi, T. Kondoh, S. Miyoshi, S. Aoki, H. Maezawa, and A. Yagishita, Nucl. Instrum. Methods A **289**, 317 (1990).
[21] T. Cho, E. Takahashi, M. Hirata, N. Yamaguchi, T. Teraji, K. Matsuda, A. Takeuchi, J. Kohagura, K. Yatsu, T. Tamano, T. Kondoh, X. W. Zhang, H. Maezawa, and S. Miyoshi, Phys. Rev. A **46**, R3024 (1992).
[22] T. Kondoh, N. Yamaguchi, T. Cho, M. Hirata, S. Miyoshi, S. Aoki, H. Maezawa, and M. Nomura, Rev. Sci. Instrum. **59**, 252 (1988).
[23] T. Cho, N. Yamaguchi, T. Kondoh, M. Hirata, S. Miyoshi, S. Aoki, H. Maezawa, and M. Nomura, Rev. Sci. Instrum. **59**, 2453 (1988); **60**, 2337 (1989).
[24] N. Yamaguchi, T. Cho, T. Kondoh, M. Hirata, S. Miyoshi, S. Aoki, H. Maezawa, and M. Nomura, Rev. Sci. Instrum. **60**, 368 (1989); **60**, 2307 (1989).

[25] M. Hirata, N. Yamaguchi, T. Cho, E. Takahashi, T. Kondoh, S. Miyoshi, S. Aoki, H. Maezawa, and A. Yagishita, Rev. Sci. Instrum. **61**, 2566 (1990).
[26] EG&G Ortec Detectors and Instruments for Nuclear Spectroscopy, pp. 1-1–1-21; S. Miyahara, Seiko EG&G Co. Ltd. (private communication) 1990, as well as M. Martini, EG&G Ortec (private communication).
[27] Tennelec Silicon Charged Particle Detector catalogue, January, 1991; M. Niki, Niki Glass Co., Ltd. Mita 3-9-7, Minato-ku 108, Japan (private communication).
[28] M. Abramovitz and I. A. Stegun, *Handbook of Mathematical Functions with Formulas, Graphs, and Mathematical Tables* (Dover, New York, 1972).
[29] Hideki Yukawa, Proc. Math. Phys. Soc. Jpn. **17**, 48 (1935).
[30] C. L. Davis, P. J. Ouseph, and M. R. O'Bryan, Rev. Sci. Instrum. **61**, 3452 (1990).